北海道大学地球物理学研究報告
Geophysical Bulletin of Hokkaido University, Sapporo, Japan
No. 69, March 2006, pp. 113−122

2-D Heterogeneous Structure in Eastern Hokkaido Inferred from *S*-wave Coda Amplification Factors

Taka'aki TAIRA
Department Terrestrial Magnetism, Carnegie Institution of Washington
and
Kiyoshi YOMOGIDA
Division of Earth and Planetary Sciences, Graduate School of Science, Hokkaido University

(Received December 21, 2005)

We examined 2-D heterogeneous structure in the eastern Hokkaido region, using the *S*-wave coda amplification factor (*CAF*) with seismic strong-motion data of Kyoshin Net (K-NET). *CAF* is defined as the spectral ratio of coda waves among different stations after corrections for source, site, and overall propagation (i.e., cada-*Q*) effects. Confirming that cada-*Q* values are nearly independent of both source and station, the site effect at each station was estimated by the coda-normalization method. The source effect was removed by taking the spectral ratio of *S*-wave coda among stations for each earthquake. We evaluated the *CAF* value of each source-station pair for three components, using 95 seismograms for five local earthquakes recorded at 21 stations of K-NET. A map of *CAF* values at the frequency band of 16 Hz shows a systematic variation, implying that heterogeneities are concentrated at the central area (Shibeccha) in the eastern Hokkaido region, manifested locally as a large degree of scattering.

I. Introduction

Understanding of small-scale heterogeneous structures in the crust is an essential key aspect in modern seismology since the pioneering work of Aki (1969). Since the density and scale of regional seismic observations have been improved significantly for the last decade, many studies have recently revealed heterogeneous structures not only in subduction zones (Revenaugh, 1995) but also at active fault zones (Nishigami, 2000) and volcanoes (Aki and Ferrazzini, 2000).

Aki and Ferrazzini (2000) found a small area with systematically large amplitude of coda waves at the summit of the Piton de la Fournaise, using the spectral amplitude of coda waves for earthquakes occurred beneath the summit. They suggested that this anomalous amplification of coda wave can be attributed to the trapped waves in the fluid-solid system of the

Piton de la Fournaise.

In the present study, we used seismograms for 13 earthquakes recorded at 21 strong-motion stations of the Kyoshin Net (K-NET) in eastern Hokkaido which was deployed all over Japan (Okada *et al.*, 2004), in order to examine a 2-D spatial variation of *S*-wave coda amplification factors (*CAF*), based on the coda spectral analysis. *CAF* is defined as the spectral amplitude ratio of coda waves among different stations after correcting the site amplification factor beneath each station as well as source and path terms (Taira and Yomogida, 2003).

II. Data and Method

To investigate a 2-D heterogeneous structure in the eastern Hokkaido region, we selected 13 earthquakes around the region in this study (Fig. 1). These earthquakes were recorded by the K-NET stations. The K-NET is a network of strong-motion accelerometers with 100 Hz sampling frequency. We analyzed seismograms in six frequency bands centered at 1, 2, 4, 8, 16, and 32 Hz with a band width of one-fourth of its centered frequency.

As mentioned in Introduction, we need to correct the site amplification factor of each station before evaluating its *CAF*. The earthquakes used in this study were divided into two data sets based on their epicentral distances (Table 1). The first data set contains eight regional earthquakes with epicentral distances equal or greater than 50 km. On the other hands, the second one includes five local earthquakes with epicentral distances less than 50 km. The first and second data sets were used to estimate the site amplification factors and the *CAF*s of all the stations, respectively. Since the epicentral distance depends on the geometry of each source-station pair, a few seismograms are not satisfied with the above criteria of epicentral distance in the two data sets. Such seismograms were removed from our present analysis.

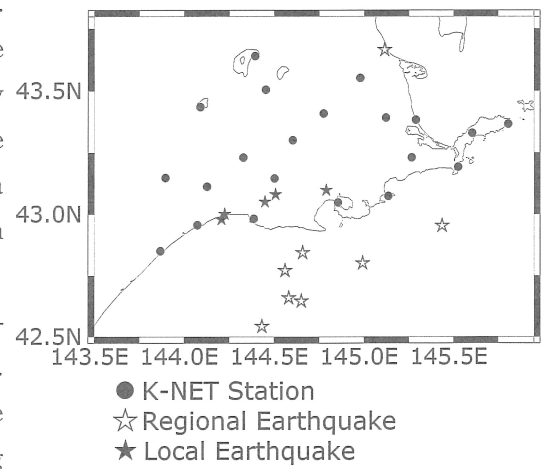

Fig. 1. Map view of K-NET stations (solid circles), and epicenters for regional (open stars) and local (solid stars) earthquakes used in this study.

Fig. 2 shows an example of accelerograms for the regional and local earthquakes. We analyzed an *S*-wave coda part with lapse time greater than twice the corresponding direct *S*-wave travel times. The time window of the coda part to be analyzed was either 20.48 or 10.24 sec. To estimate both

Table 1. Hypocentral parameters for regional and local earthquakes determined by the Japan Meteorological Agency.

Data (MM/DD/YY)	Time+	Latitude (degree)	Longitude (degree)	Depth (km)	Magnitude*
		Regional Earthquakes			
02/11/97	07:57:14.09	42.6590N	144.5815E	67.42	5.0
03/15/97	13:54:33.41	42.8435 N	144.6593 E	72.83	4.2
07/01/97	12:40:08.64	42.6458 N	144.6515 E	72.52	5.1
11/15/97	16:05:17.15	43.6567 N	145.1135 E	154.956.1	
01/03/98	03:19:56.37	42.9537 N	145.4370 E	49.56	5.0
04/09/98	14:29:31.67	42.8008 N	144.9902 E	48.32	5.0
11/15/00	23:19:30.20	42.7703 N	144.5603 E	54.88	4.5
06/07/04	13:14:14.95	42.5417 N	144.4313 E	77.76	4.9
		Local Earthquakes			
12/22/96	10:09:09.92	43.0977 N	144.7892 E	70.154.1	
06/15/97	13:54:16.92	42.9785 N	144.2073 E	97.61	5.1
11/06/97	05:04:37.93	43.0498 N	144.4483 E	116.65	4.9
06/15/99	17:13:39.94	43.0807 N	144.5068 E	93.72	4.0
04/29/03	20:43:21.64	43.0003 N	144.2252 E	97.18	4.3

+Japan Standard Time
*Japan Meteorological Agency Magnitude

site amplification factor and CAF reliably, we limited our analysis to seismograms with signal-to-noise ratio greater than 2. In this study, the signal-to-noise ratio was evaluated by the spectral ratio of the S-wave coda to noise part. The noise part was defined as a waveform before the direct P-wave of each seismogram, and its time window was 5.12 or 2.56 sec.

The S-wave coda spectral analysis used in this study was same as the one used in Taira and Yomogida (2003). Both the site amplification factor and the CAF at each station were evaluated by this spectral analysis. Note that although we do not mention the component of seismograms in the following formulae, we estimated the overall propagation (i.e., cada-Q) effect, site amplification factor, and CAF in each component separately (vertical, radial, and transverse).

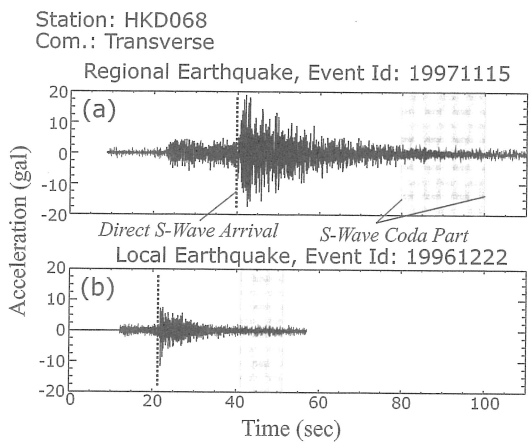

Fig. 2. An example of accelerograms for (a) regional and (b) local earthquakes in the transverse component recorded at HKD068 station. Dashed lines indicate the direct S-wave arrivals, and the analyzed S-wave coda parts are represented by gray shaded rectangles.

Assuming the single isotropic scattering model (e.g., Sato and Fehler, 1988), the time (t) and frequency (f) dependent spectral amplitude of coda wave, A_{ij}, for the i-th source at the

j-th station can be expressed by

$$A_{ij}(f, t)=S_i(f)\cdot G_j(f)\cdot C_{ij}(f, t) \qquad (1)$$

where $S_i(f)$ and $G_j(f)$ are the i-th source term and the j-th station term, respectively. $C_{ij}(f, t)$ represents the path term for the ij-th source-station pair related to the coda decay curve. Assuming the single backward scattering model (Aki and Chouet, 1975), $C_{ij}(f, t)$ can be expressed by

$$C_{ij}(f, t)\propto t^{-1}\exp\left[-\frac{\pi f t}{Q^c_{ij}(f)}\right], \qquad (2)$$

where Q^c is the quality factor of coda waves or coda-Q.

The frequency-dependent site amplification factor at each station was estimated by the coda-normalization method (Philips and Aki, 1986; Sato and Fehler, 1998). We first checked the stability of coda-Q averaged over all the S-wave coda in the eastern Hokkaido region, because the coda-normalization method to estimate site amplification factors requires that coda-Q is independent of source-station pairs. Using the eight regional earthquakes of Fig. 1, the coda-Q of each source-station pair was evaluated by a maximum likelihood method (Takahara and Yomogida, 1992).

Fig. 3 shows the coda-Q inverse of the three-component, averaged over all the regional earthquakes as well as stations, with its standard deviation. As shown in Fig. 3, coda-Q values are nearly the same among components except at the 1 Hz band. In addition, this figure indicates that coda-Q, that is, the path term $C_{ij}(f, t)$ of equation (2) is independent of locations of not only regional earthquakes but also stations, that is, $C_{ij}(f, t)\cong\tilde{C}(f, t)$ where $\tilde{C}(f, t)$ represents the average of the path terms over all the regional earthquake and station pairs.

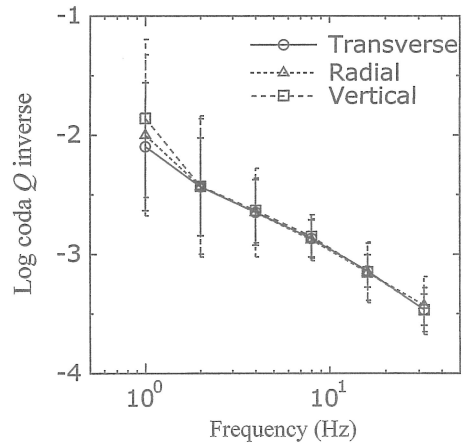

Fig. 3. Coda Q inverse values of three components in the six frequency bands (1, 2, 4, 8, 16, and 32 Hz), averaged over all regional earthquakes and 21 K-NET stations, and their standard deviations.

We then evaluated the site amplification factor at each station, by applying the coda-normalization method. The site amplification factor was determined as the spectral ratio of A_{ij} for the i-th source at the j-th station to the averaged spectral amplitude of coda wave, $\tilde{A}_i$, over all the stations:

$$\frac{A_{ij}(f,\ t)}{\tilde{A}_i(f,\ t)}=\frac{S_i(f)\cdot G_j(f)\cdot C_{ij}(f,\ t)}{S_i(f)\cdot \tilde{G}(f)\cdot \tilde{C}(f,\ t)}\cong\frac{G_j(f,)}{\tilde{G}(f)}\equiv RSAF_{ij}(f), \qquad (3)$$

where $\tilde{G}(f)$ is the average of all the station terms. The spectral ratio in equation (3) indicates the relative station term of the j-th station. Note that the source term $S_i(f)$ is assumed to be isotropic, which may be valid because we used relatively late parts of S-wave coda, as shown in Fig. 2 (e.g., Sato and Fehler, 1998). We calculated the averaged value of $RSAF$ at each station, using the eight regional earthquakes, and then defined the site amplification factor at each station as its averaged value of $RSAF$:

$$RSAF_j(f)\equiv\frac{1}{N}\sum_{i=1}^{N}RSAF_{ij}(f) \qquad (4)$$

where N is the number of the regional earthquakes.

We finally extended the coda-normalization method to the observed seismograms, in order to examine anomalous amplification of coda wave, calling it "coda amplification factor (CAF)". CAF was defined as the spectral ratio of coda wave at the j-th station to the averaged spectral amplitude of coda wave, $\tilde{A}_o$, over all the stations for a given o-th local earthquake, using the corresponding site amplification factor obtained in equation (4):

$$RSAF_j^{-1}(f)\times\frac{A_{oj}(f,\ t)}{\tilde{A}_o(f,\ t)}=\frac{S_o(f)\cdot C_{oj}(f,\ t)}{S_o(f)\cdot \tilde{C}_o(f,\ t)}=\frac{C_{oj}(f,)}{\tilde{C}_o(f)}\equiv CAF_{oj}(f), \qquad (5)$$

where $S_o(f)$ indicates the source term of the o-th local earthquake. Note that we assumed that the fluctuation of coda wave amplitude is the common within the S-wave coda part to be analyzed among stations. The second right of equation (5), therefore, becomes independent of time. The CAF value means a strength of small-scale heterogeneities in the region corresponded with the isochrone of the coda wave for a given source-station pair. While C_{ij} in equation (3) for regional earthquakes are same for all the sources and stations, C_{oj} in equation (5) for local earthquakes vary from station to station. We assumed that the former sample sufficiently large areas of heterogeneities while the latter reflect the localized heterogeneities in an area including each source and station.

III. Results and Discussion

Fig. 4 shows the distributions of the site amplification factors in the low (2 Hz) and high (16 Hz) frequency bands. Since the estimated site amplification factor at each station seems to be independent of the signal component, this figure shows the site amplification factors in the transverse component. Note that we only plotted the $RSAF$ values that satisfied the following criteria: (1) its standard deviation less than 0.5 in log scale and (2) $RSAF$ value estimated by data for at least two source-station pairs.

In the low frequency band, the site amplification factors obtained in this study strongly depend on the surface geology beneath their stations. *RSAF* values are larger than the average at the stations located on Quaternary sediment (e.g., HKD084, HKD085, and HKD086). On the other hands, *RSAF* values at basement rock (e.g., HKD072, HKD075, and HKD087) are small in general. For example, the *RSAF* values of HKD086 (Quaternary sediment site) and HKD087 (basement rock site) are about 2.5 and 0.2 times the averaged value at the 2 Hz band, respectively. Based on the observed *S*-wave coda, Philips and Aki (1986) determined the site amplification factors in central California, using a stochastic inversion method. They showed that the obtained site amplification factors at the 1.5 Hz band are mainly attributed to surface geology.

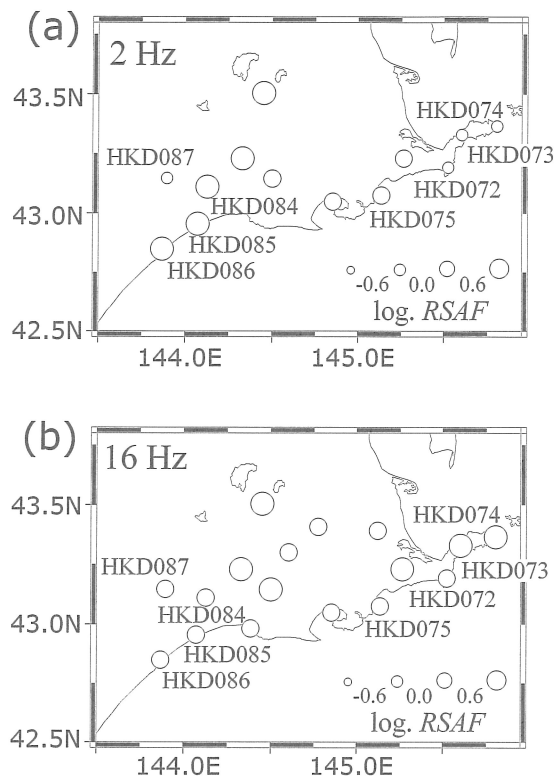

Fig. 4. Site amplification factors at K-NET stations in the transverse component at the (a) 2 and (b) 16 Hz bands. The value of site amplification factors in log scale is shown by the size, as shown in the right bottom of each panel.

In the high frequency band, the spatial variation of site amplification factors is quite different from the above case. The most obvious difference can be seen in the Nemuro region (HKD073 and HKD074) where *RSAF* values tend to increase with frequency, for example, the *RSAF* values of HKD074 at the 16 Hz band is 1.7. In contrast, at Quaternary sedimentary sites, *RSAF* values became small (0.7 times at HKD086). *RSAF* values at basement rock sites remain small (0.4 times at HKD087).

Fig. 5a shows the 2-D spatial distribution of the averaged *CAF* values at the 16 Hz band for the five regional earthquakes. We plotted the *CAF* values that satisfied the same criteria as *RSAF* for standard deviation of *CAF*s and number of source-station pairs, as mentioned above. At the central area in the eastern Hokkaido region, the *CAF* values at HKD068, HKD079, and HKD083 are larger than the averaged value at the 16 Hz band, as shown in Fig. 5a. For example, the *CAF* value of HKD068 is 7.4 times the averaged value.

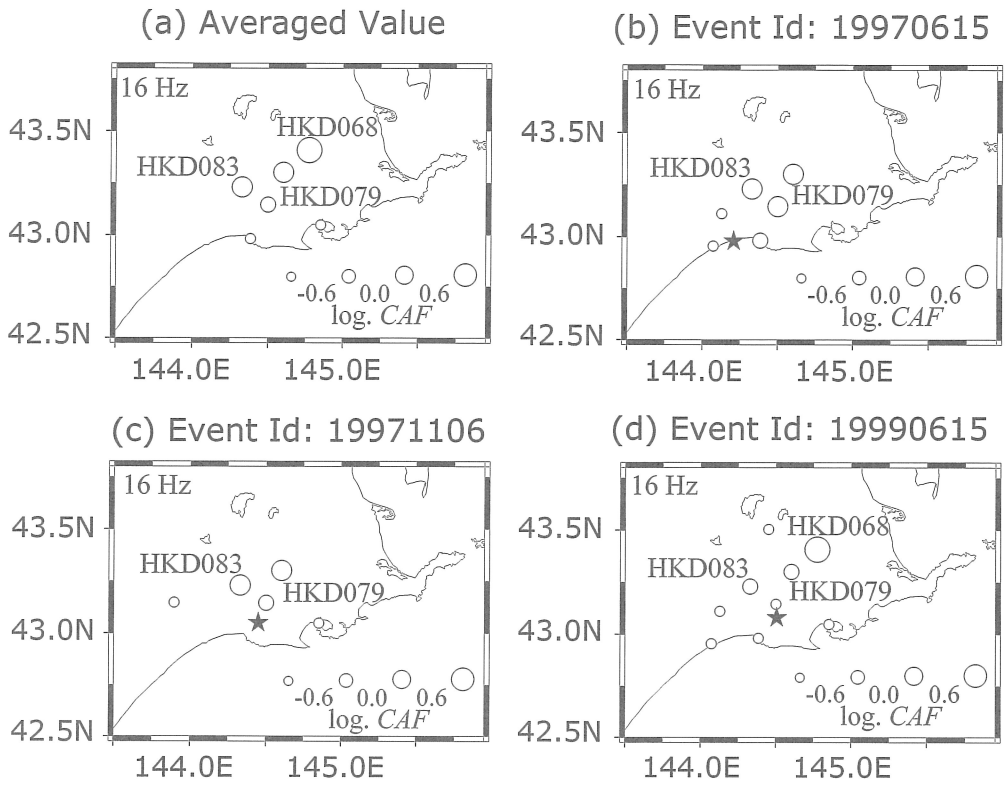

Fig. 5. Spatial variations of *CAF* values at the 16 Hz band in the transverse component. (a) The *CAF* values averaged over all local earthquakes; (b), (c), and (d) *CAF* values for one specific regional earthquake only. The event id is shown in the upper of the panel (b), (c), and (d). Also shown are the epicenters of the regional earthquakes (solid stars) on these three panels. The value of *CAF* in log scale is shown by the size, as shown in the right bottom of each panel.

This result suggests that small-scale heterogeneities in the eastern Hokkaido region should be far from random distributed ideally random.

Figs. 5b, 5c, and 5d show the estimated the maps of *CAF*s values for three specific local earthquakes. As shown in these three figures, the *CAF* values at the three stations (HKD068, HKD079, and HKD083) are relatively large regardless of local earthquake locations, which implies the large *CAF* values are mainly attributed to the small-scale heterogeneities beneath these stations rather than that near the earthquakes. Assuming the shear-wave velocity to be 4.0 km/sec (Suzuki *et al.*, 1988), the size order of the heterogeneities is around 80 m, based on the maximum scattering strength to be $kd \cong 2$ (Yomogida *et al.*, 1997), where k and d indicate the wavenumber of the *S*-wave coda and the size of the heterogeneities, respectively.

IV. Summary

We investigated the spatial variations of site amplification factors and small-scale heterogeneities in the eastern Hokkaido region, based on the *S*-wave coda spectral analysis of K-NET data. We obtained the following major results:

1. Site amplification factors at the 2 Hz band show strong dependency on surface geology, for example, the site amplification factors at basement rock sites are small while large at Quaternary sedimentary sites. On the other hands, the spatial variation of the site amplification factors at the 16 Hz band differs from that at the 2 Hz band, particularly the Nemuro region where there is a trend of the site amplification factor increasing as a function of frequency.

2. We found the systematic variation of the *CAF* values at the 16 Hz band. The *CAF* values in the central area of the studied region are relatively large independently of earthquake locations. This result implies the existence of localized small-scale heterogeneities around this area. The size order of the heterogeneities is estimated to be 80 m, assuming the shear-wave velocity to be 4.0 km/sec.

Acknowledgements The seismic data used in this study were downloaded from the K-NET web site operated by the National Research Institute for Earth Science and Disaster Prevention. The hypocentral parameters were provided by the Japan Meteorological Agency. A software package, Generic Mapping Tools (GMT), was used to plot the figures (Wessel and Smith, 1995). This work was partially supported by the Earthquake Research Institute Cooperative Research Programs (2000-B-07). The first author (T.T.) was also supported in part by a fellowship of Department of Terrestrial Magnetism, Carnegie Institution of Washington.

References

Aki, K., 1969. Analysis of seismic coda of local earthquakes as scatterered waves, *J. Geophys. Res.*, **74**, 615–631.

Aki, K., and B. Chouet, 1975. Origin of coda wave: source, attenuation, and scattering effects, *J. Geophys. Res.*, **80**, 3322–3342.

Aki, K., and V. Ferrazzini, 2000. Seismic monitoring and modeling of an active volcano for prediction, *J. Geophys. Res.*, **105**, 16,617–16,640.

Nishigami, K., 2000. Deep crustal heterogeneity along and around the San Andreas fault system in central California and its relation to the segmentation, *J. Geophys. Res.*, **105**, 7983–7998.

Okada, Y., K. Kasahara, S. Hori, K. Obara, S. Sekiguchi, H. Fujiwara and A. Yamamoto, 2004. Recent

progress of seismic observation networks in Japan —Hi-net, F-net, K-net and KiK-net—, *Earth, Planets and Space*, **56**, xv-xxviii.

Philips, W.S., and K. Aki, 1986. Site amplification of coda waves from local earthquakes in central California, *Bull. Seism. Soc. Am.*, **76**, 627—648.

Revenaugh, J., 1995. A scatterered-wave image of subduction beneath the Transverse Ranges, *Science*, **268**, 1888—1892.

Sato, H., and M.C. Fehler, 1998. *Seismic Wave Propagation and Scattering in the Heterogeneous Earth*, Springer, New York, 308pp.

Suzuki, S., T. Takanami, Y. Motoya and I. Nakanishi, 1988. A real-time automatic processing system of seismic waves for the network of Hokkaido University, *J. Seism. Soc. Japan. Ser. 2*, **41**, 359—373 (in Japanese with English abstract).

Takahara, M., and K. Yomogida, 1992. Estimation of coda *Q* using the maximum likelihood method, *Pure and Applied Geophysics*, **139**, 255—268.

Taira T., and K. Yomogida, 2003. Characteristics of small-scale heterogeneities in the Hidaka, Japan, region estimated by coda envelope level, *Bull. Seism. Soc. Am.*, **93**, 1531—1541.

Yomogida, K., R. Benites, P.M. Roberts and M. Fehler, 1997. Scattering of elastic waves in 2—D composite media II. Waveforms and spectra, *Phys. Earth Planet. Interior*, **104**, 175—192.

Wessel, P., and W.H.F. Smith, 1995. New version of the Generic Mapping Tools released, *Eos, Trans. AGU*, **76**, 329.

S波コーダ振幅から推測される北海道東部における2次元不均質構造

平　貴昭
ワシントンカーネギー研究所地磁気部門
蓬田　清
北海道大学大学院理学研究科地球惑星科学専攻

(2005年12月21日受理)

我々は，Kyoshin Net (K-NET)による強震動データのS波コーダ振幅(CAF)を用いて北海道東部における2次元不均質構造を調査した．CAFは震源，サイト，伝播(コーダQ)特性を補正した後のコーダ波による観測点間のスペクトル比として定義される．コーダQが震源および観測点に対して，ほぼ独立であることを確認し，各観測点におけるサイト特性はコーダ規格化法によって推定された．震源特性は同一の震源によるS波コーダのスペクトル比を取ることにより除去した．我々は，5個の近地地震による95個の地震波形を用いて，21点のK-NET観測点において，各震源－観測点ペアのCAFを3成分ごとに推定した．16 HzにおけるCAF分布図は系統的な変動を示し，北海道東部の中心部(標茶)において散乱の程度が局所的に大きく，不均質構造が局在していることを示唆する．